

Letter

Alloys of aluminium and tungsten in the micrometer scale

J.-C. Leclerc, Ph. Binette, M. Piché, N. McCarthy,
C. Rioux, R.J. Slobodrian*

Département de physique, de génie physique et d'optique, Université Laval, Québec G1K 7P4, Canada

Received 7 September 2006; received in revised form 4 November 2006; accepted 6 November 2006

Available online 15 December 2006

Abstract

The elements Al and W are not miscible in the liquid state. Alloys have been produced via a novel evaporation–condensation method using laser abrasion of the elements to produce vapors. The sizes of metal droplets are in the micrometer scale and scanning electron microscope images have been obtained and analyzed providing their elemental composition.

© 2006 Published by Elsevier B.V.

Keywords: Vapor deposition; Electron emission spectroscopy

1. Introduction

Alloys of elements differing vastly in their physical properties may not be possible in the liquid phase. Fig. 1 illustrates the phases of Al and W as a function of temperature and it is evident that alloys of these metals in the liquid phase are unfeasible, whereas they may become feasible in the vapor phase. The properties of the widely used Al are well known, low in density, good conductor, malleable and oxidation resistant. Tungsten is characterized by its high chemical stability, strength and rigidity. Alloys of Al–W may be qualified as exotic and may possess special properties and applications, justifying eventually a high cost of production.

In the course of studies of metallic fractal aggregates an evaporation–condensation method was developed [1] using Ohmic heating to evaporate the metals within an atmosphere of inert gas (Ar). An alloy of Al and Ag was reported in Ref. [1] evaporating simultaneously both elements. Recently lasers were used to produce the vapors [2,3] and aggregates. The basic idea consists to obtain the interaction of vapors of Al and W obtained through laser ablation in order to produce alloys. The production of such alloys pose particular problems to be discussed below.

2. General considerations

In order to obtain a successful combination of vapors it is necessary to produce them in adequate densities within a specified volume. The vastly different masses of atoms of Al and W imply that once produced by the laser beam their ranges in the argon gas shall be quite different. Collinear evaporation with a single laser beam can thus be excluded and a special geometry for the process to occur has to be determined. The one used in the experiments is based on a two-beam configuration with the metallic atom beams interacting at right angles. The velocity of an atom ejected from the metal and subjected to n collisions with the gas can be expressed as:

$$V_n = \mu^n (V_0 - V_g) + V_g \quad (1)$$

where the initial velocity is V_0 , the coefficient μ follows from classical collision energy and momentum conservation rules, V_g the thermal velocity of the element in the gas. Assuming a Maxwell initial velocity distribution it is possible to obtain an average particle energy as a function of the number of collisions, Fig. 2 shows its diagram. The initial energy E_0 diminishes rapidly and converges to the thermal energy E of the environment.

Expressing n in terms of the collision cross-section σ and the density of the medium ρ :

$$n = d \rho \sigma \quad (2)$$

* Corresponding author. Tel.: +1 418 656 3869; fax: +1 418 656 2040.
E-mail address: rjslobod@phy.ulaval.ca (R.J. Slobodrian).

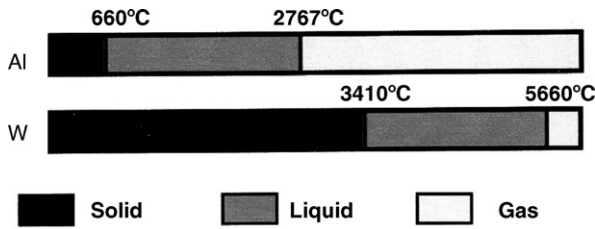


Fig. 1. Phase temperatures of Al and W.

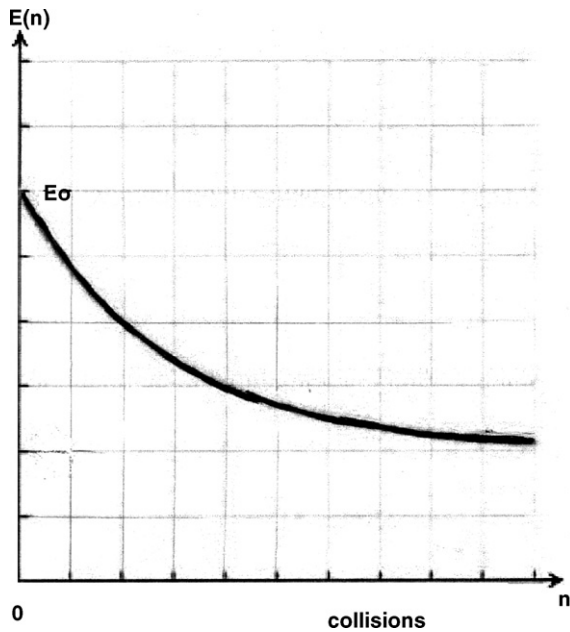


Fig. 2. Slowing down of Al atoms in Ar as a function of the number of collisions.

where d is the path in the medium. From the law of ideal gases (for Ar it is a good approximation): $\rho = P/kT$ and then it is possible to obtain the average kinetic energy in the form:

$$\langle E(P, d) \rangle = \left(\frac{3\pi}{16} \right) m [\mu^{(Pod/kT)} (V_0 - V_g) + V_0]^2 \quad (3)$$

A tri-axial representation of Eq. (3) is shown in Fig. 3. It is quite obvious that the density of atoms shall increase due to

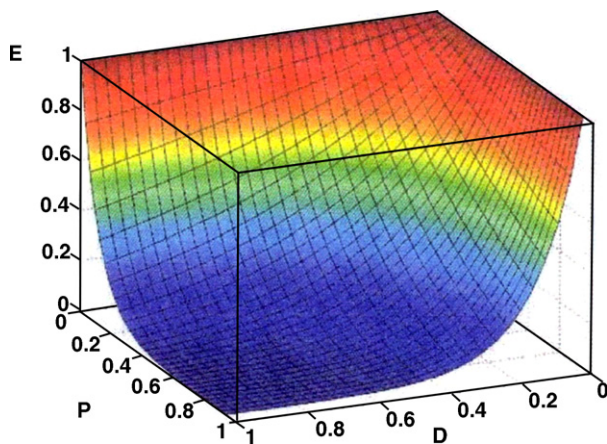


Fig. 3. Representation of Eq. (3). E : energy, P : pressure, D : path length.

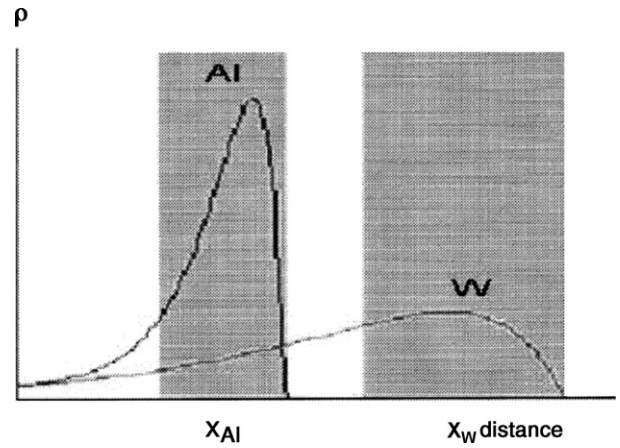


Fig. 4. Diagram of densities of Al and W atoms as a function of path length.

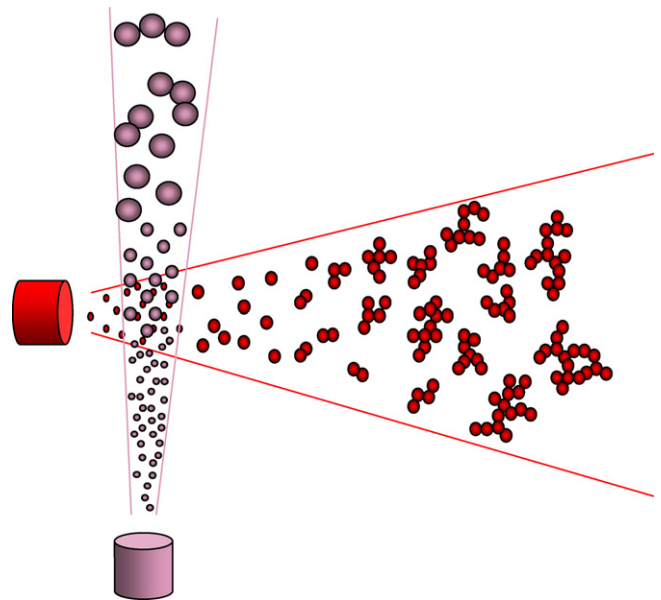


Fig. 5. Illustration of intersecting beams of atoms.

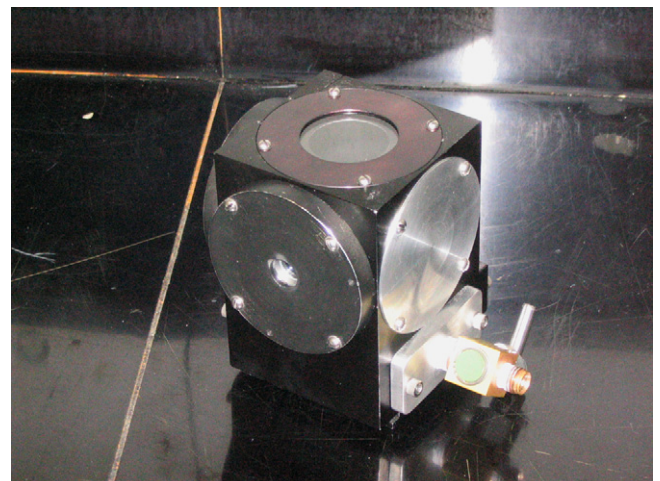


Fig. 6. The experimental cube. At the right is the gas pumping and filling valve.

Table 1

Parameters	Nominal value	Used values
Wave length (nm)	248	248
Maximum pulse energy (mJ)	450	120 and 240
Maximum mean pulse energy (W)	80	1 and 2.5
Repetition rate (pps)	200	10
Pulse duration (ns)	12 and 20	12 and 20
Beam size (mm)	8–12 × 25	8–12 × 25
Divergence of the beam (mrad)	1 × 3	1 × 3

the slowing down process. Of course there is also a diminution due to aggregation of atoms. An expression is obtained for the density as function of the path x in the gas:

$$\rho(x) = \frac{\rho_0 \langle V_0 \rangle}{[\mu^{((P/kT)\sigma)x}(V_0 - V_g) + V_g]} \times \left[1 - \frac{2}{\sqrt{3\pi m_1} [E_1^{1/2} - E_g^{1/2}] \times [\mu^{((P/kT)\sigma)x}(\langle V_0 \rangle - \langle V_g \rangle) + \langle V_g \rangle]} \right] \quad (4)$$

where the sub-index g indicates the asymptotic values for the atoms in the gas. Fig. 4 shows the actual regions of low velocity with high density and aggregation probability for Al and W indicating that a collinear geometry would fail to accomplish the alloying of Al with W. Therefore, as already mentioned, a geometry providing the projection of particles of Al at 90° with respect to W was devised illustrated schematically by Fig. 5.

3. Experimental details and results

The evaporation–condensation was carried out within a cubic chamber illustrated by Fig. 6. Five faces of the cube are actively used: the upper face bears an observation window, two adjacent lateral faces bear the metal samples of Al and

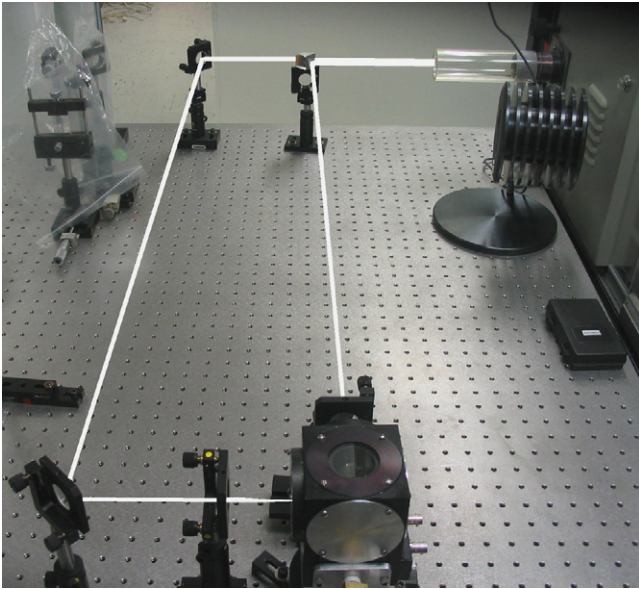


Fig. 7. The set up on the optical bench showing the intersecting beams.

Horizontal beam: Al

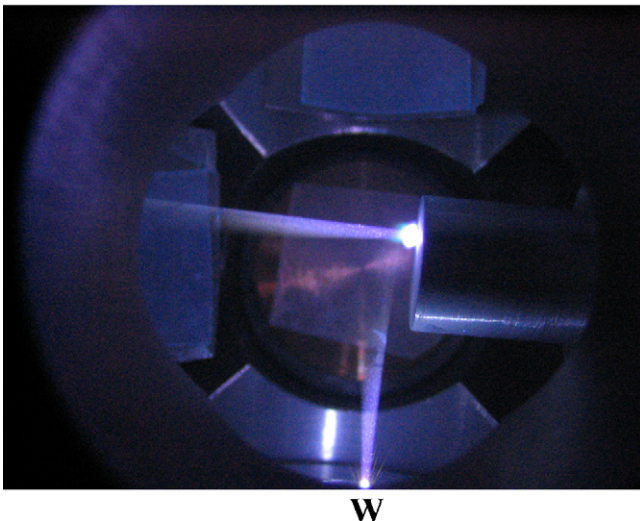


Fig. 8. Photo of the atomic beams inside the experimental cube.

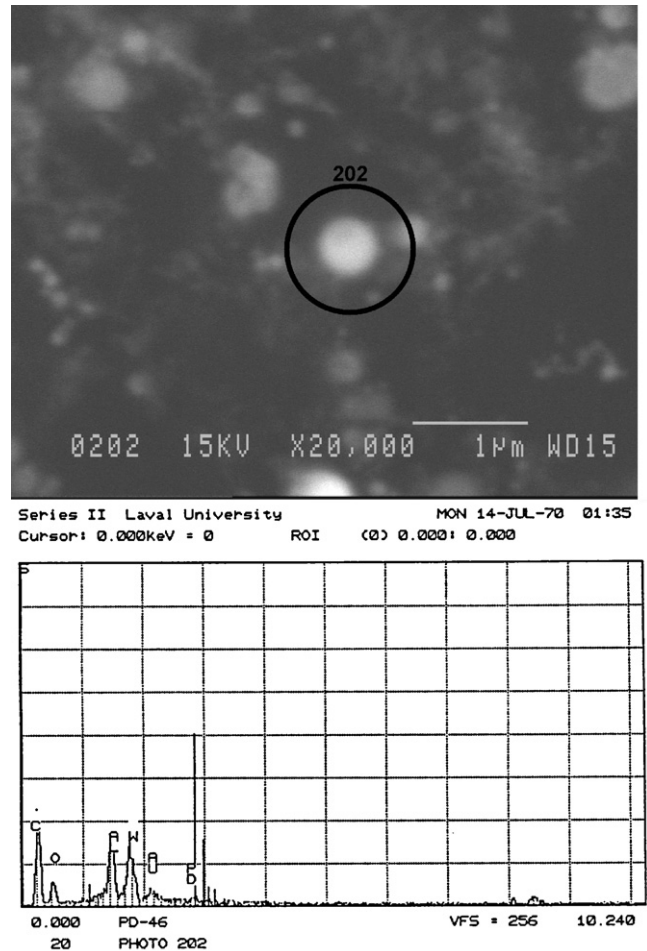


Fig. 9. SEM image and mass analysis via backscattered electrons.

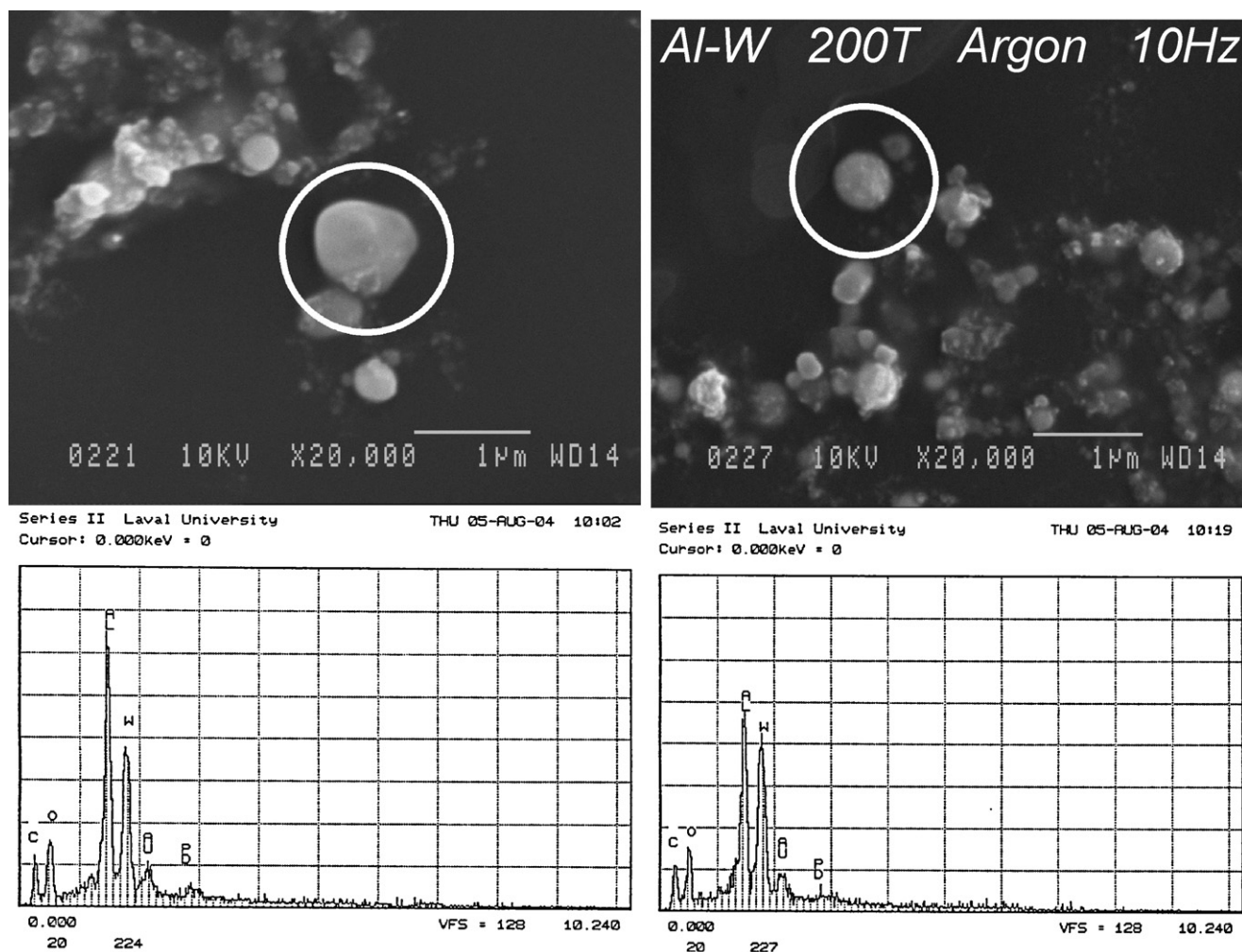


Fig. 10. SEM images and mass analyses via secondary emission electrons.

W and the remaining two allow the input of laser beams at right angles on the samples. The valve to allow the air evacuation and the Ar gas filling of the cube is visible on the right side of Fig. 6. A single laser generator was used: Excimer Pulse Master PM-848 KrF. Its characteristic parameters are given in Table 1, as well as those used during the experiments. The beam was divided into a pair of beams using a beam splitter mirror. Fig. 7 illustrates the complete experimental set up. The experimental cube is at the lower right on the figure. A photo of the cube during the operation is shown in Fig. 8 where the intersecting beams of Al and W are clearly visible.

A number of alloyed particles (14) have been observed with a scanning electron microscope (SEM). Figs. 9 and 10 show some examples of the observations, via the mass spectrometry obtained from backscattered and secondary electrons and showing the simultaneous presence of Al and W. The determination of the exact structure of the alloys is beyond the present investigation and may be the object of subsequent work.

4. Concluding remarks

According to the evidence provided here there is no limit in the possibilities provided by the evaporation condensation of

elements in order to produce alloys or combinations of atoms. It should be possible to produce alloys of multiple elements by the intersection of several atomic beams. The properties of some exotic alloys thus obtained may allow a variety of novel applications.

References

- [1] R.J. Slobodrian, C. Rioux, J.-C. Leclerc, Real and simulated low gravity fractal aggregates, in: Proceedings of the First Symposium on Microgravity Research, ESA Sp 454, vol. II, 2001, pp. 779–786, and refs therein.
- [2] M. Laliberteř, A. Boisjoli, C. Rioux, J.-C. Leclerc, M. Piché, R.J. Slobodrian, A clue for unusual metallic aggregates with monomers in the nanometer scale, *Chaos, Solitons Fractals* 22 (2004) 935–938.
- [3] A. Boisjoli, J.-C. Leclerc, M. Piché, R.J. Slobodrian, C. Rioux, S. Raymond, Optical properties of silicon micro and nanocrystals, *Microgravity Sci. Technol.* XVI-I (2005) 26–30.